

# Assessment of potential source regions of PM<sub>2.5</sub> components at a southwestern Mediterranean site

By JOSE NICOLÁS<sup>1\*</sup>, MASSIMO CHIARI<sup>2</sup>, JAVIER CRESPO<sup>1</sup>, NURIA GALINDO<sup>1</sup>, FRANCO LUCARELLI<sup>2</sup>, SILVIA NAVA<sup>2</sup> and EDUARDO YUBERO<sup>1</sup>, <sup>1</sup>Laboratory of Atmospheric Pollution (LCA), Miguel Hernández University, Av. de la Universidad s/n, 03202 Elche, Spain; <sup>2</sup>Physics Department, University of Florence and INFN, Via Sansone 1, I-50019 Sesto Fiorentino, Italy

(Manuscript received 26 March 2010; in final form 10 September 2010)

## ABSTRACT

A set of PM<sub>2.5</sub> samples ( $n = 121$ ) collected at an urban background location in Elche (in southeastern Spain) from December 2004 to November 2005 was analysed by particle-induced X-ray emission (PIXE) and ion chromatography in order to provide source identification and potential source locations. Positive matrix factorization (PMF) was used to estimate source profiles and their mass contributions. The PMF modelling identified six sources: aged sea salt (9.2%), ammonium sulphate (40.4%), soil dust related to Saharan outbreaks (13.0%), traffic 1 (18.9%), nitrate aerosol and traffic 2 (5.5%) and local soil dust (6.0%). Potential source contribution function (PSCF) was then used to identify potential source locations. Scarce influence from Mediterranean and European regions was found with the exception of the nitrate source, whose potential source areas were northern Italy and eastern France. Primary source regions for the remaining components (ammonium sulphate, soil dust-related to Saharan outbreaks and aged sea salt) with known mass contributions due to long-range transport have a marked Atlantic and North African location, primarily between Morocco and northwestern Algeria.

## 1. Introduction

In recent years the mass fraction PM<sub>2.5</sub> (particulate matter <2.5  $\mu\text{m}$  in aerodynamic diameter), also known as the fine fraction, has captured justifiable scientific interest. Several studies have shown an association between increased PM<sub>2.5</sub> concentrations and adverse health effects (Dockery et al., 1993; Schwartz and Neas, 2000) leading the European Parliament to establish legislative regulation about this fraction. European Directive 2008/50/CE establishes that an annual limit value of 25  $\mu\text{g m}^{-3}$  must be reached by January 2015.

With the objective of estimating its annual average concentrations, observing geographic and temporal variability and determining its possible sources, extensive research on a spatial scale has been conducted in Europe (Hazenkamp-von Arx et al., 2004; Querol et al., 2004; Götschi et al., 2005; Viana et al., 2007). These studies show great variability of PM<sub>2.5</sub> concentrations as well as a significant dependence on the type of environment (urban, regional, industrial or traffic). Notwithstanding, some coinciding points have been found. In general, PM<sub>2.5</sub> lev-

els tend to be higher in winter than summer. Furthermore, the primary contributions to PM<sub>2.5</sub> mass in most locations consist of organic and elemental carbon along with secondary inorganic compounds (SIC).

The chemical analysis of mass fractions in general, and particularly the fine fraction, consists in determining its primary major constituents. Different methodologies of multivariate character, like positive matrix factorization (PMF) (Paatero and Tapper, 1994), absolute principal factor analysis (APFA) (Thurston and Splenger, 1985), etc. are utilized to determine PM sources from the chemical composition. The study can be completed by obtaining the possible source origins. For this, applying techniques like potential source contribution function (PSCF) (Ashbaugh et al., 1985) or Concentration Fields (CF) (Stohl, 1996) alleviates informative deficiencies about the geographical locations of the sources. These techniques are based on combining air back-trajectory information and concentrations of the components measured at the sampling place.

Various studies have combined both techniques, obtaining comprehensive information about the particulate matter sources and origins at certain locations like the United States (Kim et al., 2003; Hwang and Hopke, 2007), areas in the eastern (Doğan et al., 2008; Koçak et al., 2009) and western Mediterranean (Salvador et al., 2004). Salvador et al. (2008) show how potential

\*Corresponding author.

e-mail: j.nicolas@umh.es

DOI: 10.1111/j.1600-0889.2010.00510.x

source areas can be different depending upon the mass fraction analysed, and that for the same mass fraction the geographic location of such areas can differ over time.

This research is presented with the aim of determining and characterizing PM<sub>2.5</sub> sources utilizing PMF, and the posterior application of PSCF to identify the potential source locations. The study takes place in an urban environment on the western Mediterranean coast. Because of this geographic location any possible European, Mediterranean, Atlantic and above all North African influences will be evaluated as potential source regions, which due to particular synoptic situations favour long distance transport and contribute to the concentration value of the fine fraction at the sampling point.

## 2. Features of the study area

PM<sub>2.5</sub> concentration and composition was studied in the urban area of Elche (38°16'N; 0°41.5'W), a city with ~180 000 inhabitants in southeastern Spain. Elche is located ~10 km from the Mediterranean coast. The city of Elche has a Mediterranean climate with mild winters and moderately hot summers. The prevailing wind regime in the zone during summer is the sea breeze, while the typical synoptic situations in winter have an Atlantic origin. Its scarce annual precipitation, between 150–250 mm, is concentrated primarily in spring and fall, and sparse ground vegetation in the region classifies the nearby surroundings as semiarid.

Southeast Spain is one of the areas along the western Mediterranean coast that receives particulate matter contributions with a higher frequency due to its proximity to the African continent. In fact, approximately 16% of the air masses arriving annually to the study area have North African origins. These outbreaks occur with the greatest frequency and intensity from spring to early fall. Events also occur during winter and early spring, although with a lower frequency, and this type of transport is not common in November or December. Usually between 16 and 19 episodes take place annually (Querol et al., 2008). Other wind directions transporting air pollution to the study area are Atlantic (55%), European (14%), Regional (transport regimen dominated by sea–land breeze recirculations) (11%) and Mediterranean (4%) (Querol et al., 2008).

It is important to emphasize the significant influence that winter pollution episodes have upon PM<sub>2.5</sub> within the study area (Galindo et al., 2008). These are mostly related to the presence of high-pressure systems over the Iberian Peninsula that promote highly stable atmospheric conditions. Under this meteorological situation, important decreases in the mixing layer or even thermal inversions occur, which favour the accumulation of pollutants from local sources.

Road traffic (more than 130 000 motor vehicles licensed in the study period) constitutes the main source of anthropogenic pollution in the urban area. The footwear industry in Elche is significant, although not all stages of manufacturing are per-

formed within the city. Shoe tinting and dyeing of the leather comprising the footwear is not usually performed in Elche; it arrives from third countries already prepared. In general, the work conducted locally is the cutting and assembly of pieces with adhesive solvents and the final finish of the products, which can generate Volatile Organic Compounds (VOCs), not measured in this study. Based on this, this industry does not represent a local source of suspended particles to consider.

## 3. Methodology

### 3.1. Sampling

PM<sub>2.5</sub> samples were collected daily between December 2004 and December 2005, and 121 are analysed in this work. The selection criteria of the samples chosen for subsequent compositional analysis is based on achieving broad representativeness, both in the general processes and in the possible events, anthropogenic and natural, that affect PM<sub>2.5</sub> in the sampling area during the study period. Furthermore, in an effort to prevent skewing the results, the number of samples analysed per month was very similar.

The particulate matter samples were collected on 47 mm diameter quartz fiber filters by a low volume LVS.3.1 CEN EN 12341 reference sampler. The sampler was located at an urban background location, 12 m above ground level on a building roof. Total mass concentrations were obtained gravimetrically using an Ohaus AP250D microbalance (sensitivity 10 µg) after conditioning the filters in a climate-controlled room at a temperature of 20 ± 1 °C and humidity of 50 ± 5%. The samples, once weighed, were kept in a refrigerator (4 °C) until their chemical analysis to avoid losses from volatilization.

### 3.2. Analytical techniques

The samples were analysed by particle-induced X-ray emission (PIXE) at the 3 MV Tandatron accelerator of the LABEC laboratory of the National Institute of Nuclear Physics (INFN) in Florence, Italy. An external beam facility fully dedicated to measuring elemental composition of atmospheric aerosols has been installed there. Detailed technical specifications of the setup and analysis conditions are reported in Calzolari et al. (2006). Here we will only briefly mention that thanks to the combined use of a Silicon Drift Detector (SDD), together with a traditional Si(Li) detector for the collection of low- and high-energy X-rays, respectively, it is possible to analyse quartz samples with measurements lasting only a few minutes (~5 min) to obtain elemental concentrations for all elements with atomic number  $Z > 10$ . However, due to the high silicon content in the filters themselves, it is not possible to measure the Si concentrations in the samples.

Since PIXE is a non-destructive technique, the same samples were additionally analysed by ion chromatography (IC) at

the Laboratory of Atmospheric Pollution (LCA) of the Miguel Hernández University (Elche, Spain) to complete the sample composition. The ion chromatograph used was a DIONEX® model DX-120 with chemical autosuppression. An anionic column model AS9-HC and a cation column CS12A were used, both 250 mm in length and 4 mm in diameter. The ions determined in the samples were  $\text{SO}_4^{2-}$ ,  $\text{NO}_3^-$  and  $\text{NH}_4^+$ .

For PIXE analysis, minimum detection limits (MDL), at  $1\sigma$  level, are  $\sim 10 \text{ ng m}^{-3}$  for low-Z elements and  $\sim 1 \text{ ng m}^{-3}$  (or below) for medium-high Z elements, while the uncertainty of the elemental concentrations is in the range of 2–20%. For IC analysis, the MDL were  $0.01 \mu\text{g m}^{-3}$  ( $\text{NH}_4^+$ ),  $0.06 \mu\text{g m}^{-3}$  ( $\text{NO}_3^-$ ) and  $0.05 \mu\text{g m}^{-3}$  ( $\text{SO}_4^{2-}$ ).

### 3.3. Meteorological analysis

Atmospheric dynamics and the detection of African dust outbreaks were performed by satellite images provided by the NASA SeaWiFS project to detect dust plumes (McClain et al., 1998), two dust prediction models, the NAAPS model from the Naval Research Laboratory and the ICOD/DREAM model (Nickovic et al., 2001) and backtrajectory calculation programs, HYSPLIT model (Draxler and Rolph, 2003). NCEP meteorological maps (Kalnay et al., 1996) were also used.

To verify the winter pollution episodes, the CBL (convective boundary layer) height was determined using the parcel method. Meteorological soundings from the University of Wyoming, <http://weather.uwyo.edu/upperair/sounding.html>, were utilized. The soundings gathered at a station located near the city of Murcia ( $37^\circ 59' \text{ N}$ ;  $1^\circ 7' \text{ W}$ ; 62 m a.s.l.), a location near our sampling site, were consulted. Meteorological data series from the Environmental Surveillance Network of the regional Government of Valencia were also used.

### 3.4. Data treatment

**3.4.1. Positive matrix factorization.** The PMF model developed by Paatero and Tapper (1994) and Paatero (2004) is a method based on solving the factor analysis problem by least squares using a data point weighing method, which uses estimates of the data uncertainties to provide optimum data point scaling. A conventional factor analysis model can be written as

$$\mathbf{X} = \mathbf{GF} + \mathbf{E}, \quad (1)$$

where  $\mathbf{X}$  is the known  $n \times m$  matrix of the  $m$  measured elements or chemical species in  $n$  samples.  $\mathbf{G}$  is an  $n \times p$  matrix of source contributions to the samples (time variations).  $\mathbf{F}$  is a  $p \times m$  matrix of source compositions (source profiles).  $\mathbf{E}$  is defined as a residual matrix, that is, the difference between the measurement  $\mathbf{X}$  and the model  $\mathbf{Y}$  as a function of factors  $\mathbf{G}$  and  $\mathbf{F}$ .

$$e_{ij} = x_{ij} - y_{ij} = x_{ij} - \sum_{k=1}^p g_{ik} f_{kj}, \quad (2)$$

where  $i = 1, \dots, n$  samples;  $j = 1, \dots, m$  elements or chemical species;  $k = 1, \dots, p$  sources.

The PMF objective is to minimize the sum of the squares of the inversely weighed residuals with uncertainty estimates of the data points. Furthermore, PMF constrains all the elements of  $\mathbf{G}$  and  $\mathbf{F}$  to be non-negative, meaning that sources cannot have negative species concentration ( $f_{kj} \geq 0$ ), and the sample cannot have a negative source contribution ( $g_{ik} \geq 0$ ). The objective function to be minimized,  $Q(\mathbf{E})$ , is defined as

$$Q(\mathbf{E}) = \sum_{i=1}^m \sum_{j=1}^n \left[ \frac{e_{ij}}{s_{ij}} \right]^2, \quad (3)$$

where  $s_{ij}$  is an uncertainty estimate in the  $j$ -th element measured in the  $i$ -th sample. The solution for eq. (3) is obtained by the PMF2 algorithm, in which both matrices  $\mathbf{G}$  and  $\mathbf{F}$  are adjusted in each iteration step. The process continues until convergence occurs (Paatero, 1997).

The Polissar et al. (1998) procedure was used to assign measured data and associated uncertainties as the PMF input data. The concentration values were used for the measured data and the sum of the analytical uncertainty, as well as 1/3 of the detection limit value was used as the overall uncertainty assigned to each measured value. Values below the detection limit were replaced by half of the detection limit values, and their overall uncertainties were set at the sum of 1/2 of the average detection limits for this element and 1/3 of the detection limit values.

Since the chemical analysis was not sufficiently detailed (we are not sure that the unmeasured species can either be assumed to be strongly correlated to measured species or represent sources that add negligible mass to the particulate matter samples), the measured particulate matter mass concentration was included as an independent variable in the PMF model to directly obtain the mass apportionment without the usual multilinear regression. However, we also performed the analysis including the PM mass as dependent variable (with MLRA). The results obtained were very similar to those obtained using the  $\text{PM}_{2.5}$  as an independent variable. No negative regression coefficients were obtained.

The estimated uncertainties of  $\text{PM}_{2.5}$  mass concentrations were set at four times their values so that the large uncertainties decreased their weight in the model fit. When the measured particulate matter mass concentration is used as a variable, the PMF apportions a mass concentration for each source according to its temporal variation. The PMF modelling results were normalized by the apportioned particulate matter mass concentration so that the quantitative source contributions for each source were obtained. Specifically,

$$x_{ij} = \sum_{k=1}^p (c_k g_{ik}) \left( \frac{f_{kj}}{c_k} \right), \quad (4)$$

where  $c_k$  is the directly apportioned mass concentration by PMF for the  $k$ -th source (Kim et al., 2004).

**3.4.2. PSCF.** PSCF model statistics count each trajectory segment endpoint that terminates within that grid cell. The probability of an event at the receptor site is related to that cell. The PSCF value can be interpreted as the conditional probability that concentrations larger than a given criterion value are related to the passage of air parcels through the cell during transport to the receptor site. Cells for which high PSCF values are calculated result from the arrival of air parcels at a receptor site with pollutant concentration higher than a given value observed at the site. These cells are an indication of areas of high potential contributions to the pollution at a receptor site.

In this study, the PSCF values were calculated using the source contributions and backward trajectories produced by the hybrid single particle Lagrangian integrated trajectory (HYSPLIT) model. PSCF<sub>ij</sub> is defined as

$$\text{PSCF}_{ij} = m_{ij}/n_{ij}, \quad (5)$$

where  $n_{ij}$  is the total number of endpoints that fall in the  $ij$ -th cell and  $m_{ij}$  is the number of endpoints in the same cell that are associated with samples that exceeded the threshold criterion. In this case, the criterion values for each parameter are the 75th percentile values for the whole period. The fact of requiring a sufficiently elevated critical value (75th percentile) is due to the sampling site being located in an urban environment affected by local traffic emission, because of which this criterion is required in order to better perceive the external influences to PM<sub>2.5</sub> (Salvador et al., 2004).

Four-day backward trajectories were calculated at 18:00 UTC at a height of 1500 m a.s.l. This height can be considered a representative height of the mean transport wind at synoptic scale within the upper boundary layer. The total number of endpoints was 23 981 and the geophysical region covered by the trajectories was divided into 1886 grid cells of  $1^\circ \times 1^\circ$  latitude and longitude. Therefore, there is an average of 13 trajectory endpoints per cell. In order to reduce the effect of small values of  $n_{ij}$  that result in high PSCF values with high uncertainties, an arbitrary weight function  $W(n_{ij})$  was multiplied into the PSCF value to better reflect the uncertainties in the values for these cells (Polissar et al., 2001). The weight function used in this work is defined as follows:

$$W(n_{ij}) = \begin{cases} 1 & n_{ij} > 13 \\ \frac{n_{ij}}{13} & n_{ij} \leq 13 \end{cases} \quad (6)$$

The weighting extends until  $n_{ij} = 13$ , which corresponds to the mean number of endpoints per cell. This criterion in the selection of this type of weight function can be seen in Plaisance et al. (1996). However, other procedures exist when considering this function. In this way the value  $W(n_{ij}) = 1$  can be assigned when the total number of endpoints per specific cell was less than about two (Hwang and Hopke, 2007) or three (Ara Begum et al., 2005) times the average value of the endpoints per cell.

*Table 1.* Mean values, standard deviations, minimums and maximums of the elemental and ionic concentrations ( $\text{ng m}^{-3}$ ) and percentage of valid samples with concentrations above the MDL

Element/Ion	% Valid samples	Mean	$\sigma$	Max.	Min.
PM <sub>2.5</sub>	100	15334	9134	54600	3600
NO <sub>3</sub> <sup>-</sup>	100	1356	2212	15504	97
SO <sub>4</sub> <sup>-2</sup>	100	3835	2952	15949	417
NH <sub>4</sub> <sup>+</sup>	100	1634	1407	6730	65
Na	78	276	109	541	128
Mg	89	24	12	55	7
Al	100	293	67	534	197
Cl	60	180	223	1134	40
K	97	223	197	1271	70
Ca	100	232	122	721	28
Ti	55	9	5	27	4
V	64	9	5	26	3
Mn	63	3	1	9	2
Fe	100	61	36	184	21
Ni	96	3	2	11	1
Cu	100	6	6	50	2
Zn	100	11	12	80	2
Br	96	4	2	12	1
Pb	75	7	5	37	2

## 4. Results and discussion

### 4.1. PM<sub>2.5</sub> composition: mean values of the concentrations and influence of events

Table 1 shows the average concentrations of the ionic and elemental components of PM<sub>2.5</sub> obtained from 121 samples during the study period. Some elements analysed, like Cr, As, Sr and Se, are not included because the percentages of valid samples (concentrations superior to the corresponding MDL) are less than 50%.

The PM<sub>2.5</sub> annual average value,  $15.3 \mu\text{g m}^{-3}$ , is below that found at other Spanish urban background stations, whose range of values oscillates between  $20\text{--}30 \mu\text{g m}^{-3}$  (Querol et al., 2004; Querol et al., 2008). However, the contribution from SIC to the PM<sub>2.5</sub> mass ( $\sim 44\%$ ) is superior to the percentages obtained at these types of stations in Spain ( $20\text{--}33\%$ ) (Querol et al., 2008) and even Europe (Querol et al., 2004). This result demonstrates the importance of these compounds within the study area.

PM<sub>2.5</sub> seasonal tendency is determined by maximums in winter due to episodes of local atmospheric stagnation, and by relative maximums in spring and summer. The PM<sub>2.5</sub> summer maximums are primarily produced by an increase in SICs. This SIC growth is due to greater photochemical activity, a higher frequency of recirculation episodes (Viana et al., 2007), and frequent transport of particulate matter from North Africa. Both Saharan dust intrusions and local pollution episodes have an important impact on PM<sub>2.5</sub> concentrations; however, changes in

Table 2. Average concentration ( $\text{ng m}^{-3}$ ) of ionic and elemental  $\text{PM}_{2.5}$  constituents on African outbreak days, stagnant days and days without events

Element/ Ion	Without events ( $n = 80$ )	Stagnant episode ( $n = 13$ )	African outbreak ( $n = 28$ )
$\text{PM}_{2.5}$	10104	30032	20704
$\text{NO}_3^-$	570	5819	1500
$\text{SO}_4^{2-}$	2374	4017	6389
$\text{NH}_4^+$	882	3045	2569
Na	171	156	326
Mg	17	16	33
Al	278	301	336
Cl	66	392	91
K	90	339	217
Ca	223	268	242
Ti	5	7	10
V	4	12	10
Mn	2	4	3
Fe	46	85	89
Ni	3	5	4
Cu	5	15	4
Zn	8	28	9
Br	3	8	4
Pb	4	14	7

$\text{PM}_{2.5}$  composition are different under each type of event. Table 2 presents average concentrations obtained during these episodes, and compares them with those obtained when these events are not considered.

Both events notably increase SIC concentrations, and while during intrusion periods the greatest increase occurs in  $\text{SO}_4^{2-}$  levels, it is during accumulation periods that  $\text{NO}_3^-$  increases its value 10 times. The formation of fine sulphate during intrusion periods has been previously observed (Galindo et al., 2008) and is possibly due to preferential oxidation of  $\text{SO}_2$  on small particles due to their greater specific surface. The contribution of fine ammonium nitrate to  $\text{PM}_{2.5}$  peaks registered under winter atmospheric stability conditions has been reported in some previous studies (Schaap et al., 2004; Galindo et al., 2008; Perrino et al., 2008). Particulate ammonium nitrate is semivolatile and exists in equilibrium with gas phase nitric acid and ammonia. The particle phase is favoured by the low temperatures and high relative humidities (Kuhns et al., 2003) characteristic of high atmospheric stability periods.

The most important increases in elements typically anthropogenic, like V, Cu, Zn or Pb take place during stagnation periods. In this case, Cl stands out, ostensibly increasing its concentration, and confirming the non-marine origin of fine chlorine in urban environments.

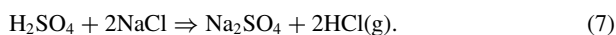
Elevated concentrations of crustal elements, especially Ti and Fe, occur during Saharan dust intrusions. The greatest repercussion logically presents itself in crustal elements like Ti or Fe,

but not Ca, whose concentration practically remains constant. Because of this, these two elements can be considered as the principal tracers of this type of transport for the fine fraction in the study area. The value of these elements upon the  $\text{PM}_{10}$  fraction as tracers in the study area has already been observed (Nicolás et al., 2008). The average ratios of these elements between African and non-African episodes are 2.0 for Ti and 1.9 for Fe. Even so, these values are lower than those obtained at other areas in the Iberian Peninsula, 6.5 and 4.7 for Ti and Fe, respectively (Viana et al., 2007). Table 2 also shows how during these events some anthropic elements like Pb or V increase their concentrations with respect to days without events. This circumstance could be due to these elements being incorporated into Saharan dust plumes as they pass over urban or industrial areas until arriving at the sampling point (Doğan et al., 2008).

#### 4.2. $\text{PM}_{2.5}$ source profiles by PMF

PMF identified six sources for the  $\text{PM}_{2.5}$  fraction. Figure 1 illustrates the identified source profiles and explained variation (EV) for each element/ion in each source (source profiles show which elements and ions make up a certain PM source, and also indicate the contribution of these elements/ions in this source. EV provides an indication of which sources are most responsible for explaining the variation in each particular chemical species used in the PMF analysis). Figure 2 shows time-series plots of daily contributions to  $\text{PM}_{2.5}$  mass concentration from each source. Additionally, the figure presents the percentage contribution from each source to  $\text{PM}_{2.5}$  mass, as well for the summer ( $n = 60$ ) and winter ( $n = 61$ ) periods. The months with average monthly temperature exceeding  $20^\circ\text{C}$  were chosen for the summer period (from May to September), with those remaining considered as cold months.

The first source is of marine origin characterized by the presence of Na, Mg and  $\text{SO}_4^{2-}$ . This is usually called ‘aged sea salt’ due to the lack of Cl (Hwang and Hopke, 2007). The lack of Cl in this source indicates that some type of reaction is occurring to make it disappear. This reaction might be responsible for the Cl disappearance:



In this case, particles rich in Na are obtained as a result. If the source profile is observed, important quantities of  $\text{SO}_4^{2-}$  appear, suggesting that the reaction (7) is occurring. The non-inclusion of  $\text{NO}_3^-$  in the aged sea salt source is unusual; nevertheless, fine nitrate concentrations in the study zone are very low during the summer season ( $<0.6 \mu\text{g m}^{-3}$ , seasonal minimum) while  $\text{SO}_4^{2-}$  levels are highest ( $>5.0 \mu\text{g m}^{-3}$ , seasonal peak). This is possibly the reason why the model does not associate the  $\text{NO}_3^-$  with this source.

Temporal evolution of this source presents minimum values during winter months because sea breezes are rare at this time of the year. During the rest of the year, the concentrations of this

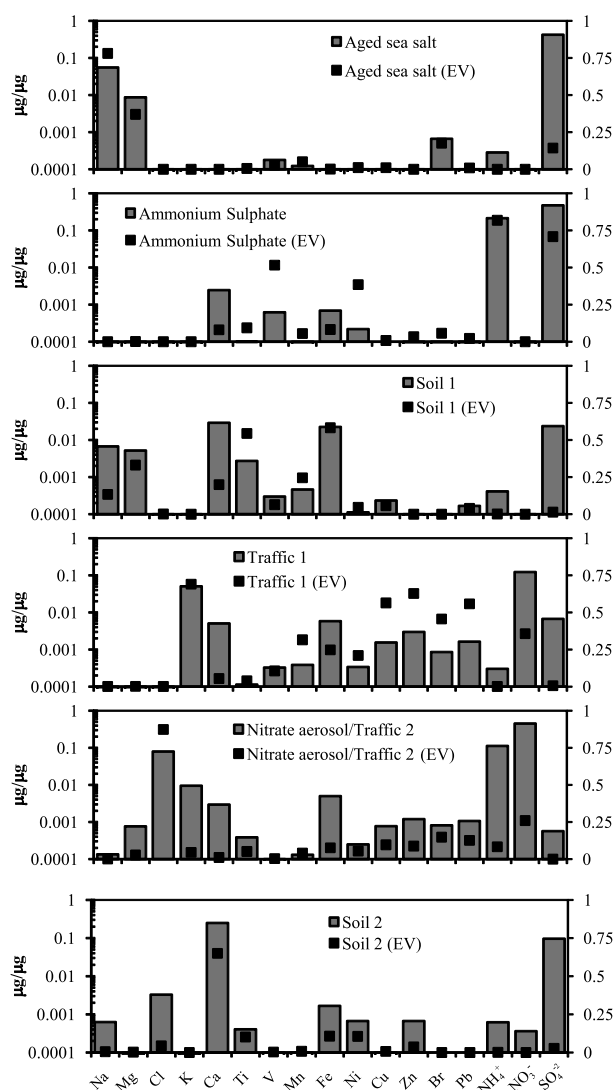


Fig. 1. Source profiles (value  $\pm$  explained variation) of the identified PM<sub>2.5</sub> sources measured at Elche. (Left axis: value of ion/element in the source, represented by grey bars. Right axis: explained variation, represented by dark squares).

source are much more elevated. The effects of marine breezes (SE winds) are noticed at the sampling point on approximately 40% of the days of the year. They are, however, mainly concentrated during the months of spring and summer, making up 75% of the total. For its part, Atlantic advection can also be responsible for some peaks registered by this source, above all those occurring in fall.

The ammonium sulphate source is primarily formed from  $\text{SO}_4^{2-}$  and  $\text{NH}_4^+$ , indicating that  $(\text{NH}_4)_2\text{SO}_4$  is the primary compound of this source. The presence of V in this source indicates that this factor also has a local contribution of combustion sources. The seasonal evolution of this source is characterized by a clear maximum in summer due to greater  $\text{SO}_2$  oxidation

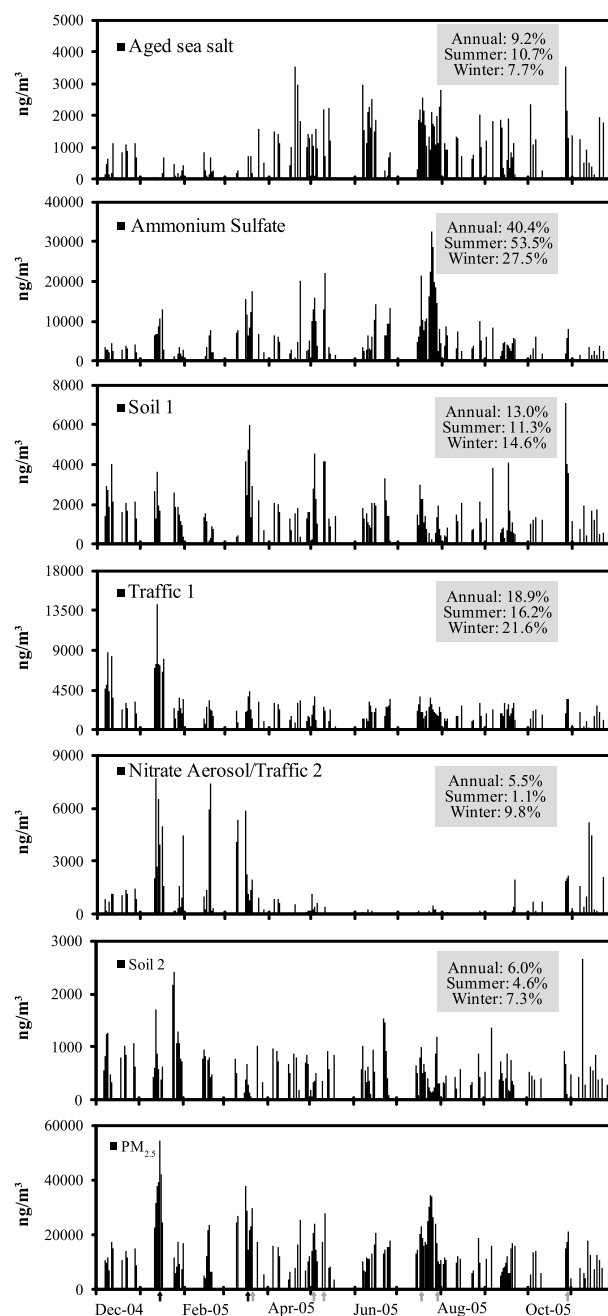


Fig. 2. Temporal variation of source contribution for the Elche site using the PMF model. The arrows denote the periods in which the main Saharan dust outbreaks (grey arrows) and high atmospheric stability conditions (black arrows) occurred.

from high radiation and temperature levels reached during this time of the year in the study area. This is the source contributing the greatest percentage to the PM<sub>2.5</sub> value, 40.4%, with a quite significant oscillation between the winter (27.5%) and summer (53.5%) periods, proof of its dependence upon solar radiation.

The third source, soil 1, is characterized by crustal elements (Ti, Ca, Fe and Mn) as well as Na and Mg. This source includes contributions of North African dust. This identification is made based on three facts: (1) the soil source presents a high correlation with Ti, a clear marker of African transport episodes as explained earlier; (2) Na and Mg, elements integrated in this source, can be collected by the Saharan plume along its trajectory over water and arrive at the sampling point and (3) if the temporal evolution is observed, marked peaks appear, coinciding with the predicted intrusions previously identified (see grey arrows in Fig. 2).

The profiles presented by the two following factors show traffic to be the primary origin of both of them. Nevertheless, slight differences appear which profile the 'traffic 1' factor as a source related more with non-exhaust particulate matter from road traffic (primary traffic) than the second, 'nitrate aerosol/traffic 2' (secondary traffic). Even so, establishing clear differences between both factors is complex because some common elements are present in both of them. Primarily these are elements like Ca and Fe, which are typical road dust tracers (Thorpe and Harrison, 2008). For their part, Cu, Zn and Pb are usually related with brake linings, and additionally Zn is emitted by tyre wear (Sternbeck et al., 2002).

Nitrate aerosol/traffic 2 presents some characteristics distinguishing it from the first traffic source, and gives it a character related more with traffic exhaust, as already mentioned. In secondary traffic, there is the presence of  $\text{NO}_3^-$  and  $\text{NH}_4^+$ .  $\text{NO}_3^-$  derives from gas to particle conversion processes of products in  $\text{NO}_x$  oxidation, and it is thought to result mainly from vehicle exhaust (Almeida et al., 2006).  $\text{NO}_3^-$  reacts with  $\text{NH}_4^+$ , forming  $\text{NH}_4\text{NO}_3$ , and is unstable at high temperatures. This thermal property is evident in the temporal evolution and in the differences between seasonal contributions, 1.1% in summer and 9.8% in winter (see Fig. 2). Also, this second traffic source includes chlorine as a featured element. In fact, the EV in this source rises above 0.8. Cl is primarily emitted in the form of HCl, later reacting with ammonia to form  $\text{NH}_4\text{Cl}$  in the fine mode (Kaneyasu et al., 1999).

The main maximums of the two traffic components usually occur during periods of atmospheric stagnation (see the black arrows in Fig. 2). This is due to the predominantly local origins of the elements/compounds constituting these sources.

Finally, soil 2, the last source, is fundamentally marked by the presence of Ca. Ca predominates due to the soil in the study area being limestone. Contrary to soil 1, this may be the result of local and regional resuspension by wind and convective processes, and soil 2 accounts for 6% of the total  $\text{PM}_{2.5}$  mass. One potential source of calcium in the study area might be the cement industries that are located 25–30 km to the NE, but this possibility is minor due to the significantly low frequencies with which air arriving in the city originates from that direction. NW winds predominate, with the exception of SE sea breezes in the summer. This does not mean to say that no contribution exists,

Table 3. Pearson correlation coefficients ( $r$ ) values between  $\text{PM}_{2.5}$  and sources daily concentrations

Period	Ammonium sulphate	Traffic 1	Secondary nitrate/traffic 2
Winter	0.78	0.58	0.68
Summer	0.94	0.45	0.19
Annual	0.71	0.53	0.54

although we believe that its contribution to the annual total is not important.

The annual unexplained concentration percentage was 7%.

The primary factors modulating the observed temporal variation in  $\text{PM}_{2.5}$  concentrations are traffic 1, traffic 2/secondary nitrate and above all ammonium sulphate. Table 3 presents the Pearson ( $r$ ) coefficient obtained by correlating the daily values of these sources against those of  $\text{PM}_{2.5}$ .

#### 4.3. PSCF analysis

Figure 3 shows maps with PSCF values for higher concentrations (above the 75th percentile) of ammonium sulphate, secondary nitrate/traffic 2, soil 1 and aged sea salt recorded in Elche. The maps corresponding to the two remaining sources, traffic 1 and soil 2, are not shown. These maps present the highest PSCF values below 0.45, located in the Mediterranean Sea near the southeast Spanish coast. These sources, above all traffic 1, are sensitive to high pollution episodes like shown in Fig. 2, and these episodes have a local origin.

The marine source presents a well-defined geographic area with elevated PSCF values, superior to 0.55. This area is located in the Atlantic between the latitudes 32–39°N. The source zone has a maximum value above 0.65 between the longitudes 12–16°W, just north of the Canary Islands (Fig. 3a). Air masses arriving from these regions are primarily facilitated by Atlantic advection associated with frontal systems. On occasions, this is also due to the presence of high-pressure systems in northwestern Africa.

The highest PSCF values for ammonium sulphate are located in the Atlantic (to the southwest of the Iberian Peninsula) and north of Morocco (Fig. 3b). It is possible that the elevated levels of this source coming from these geographic areas are related with Saharan intrusion periods arriving at the study zone from the Atlantic. The formation of fine sulphate during intrusions of North African air masses has already been mentioned. The fact that more than 1/3 of the days that the  $(\text{NH}_4)_2\text{SO}_4$  exceeds the 75th percentile coincide with those of soil 1 supports the previous hypothesis. These days predominantly take place during the summer season.

The predominant meteorological pattern at 850 mb from which air masses reach the study area from the regions having the highest PSCF for this source is that of an anticyclone

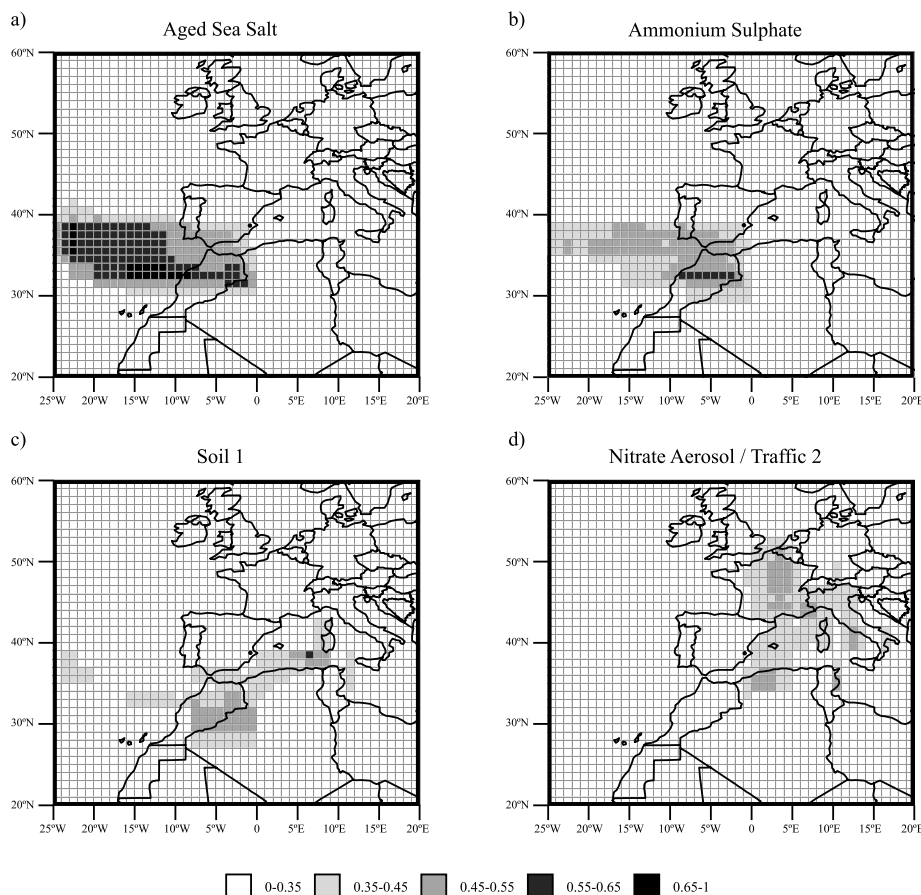


Fig. 3. PSCF values for: (a) aged sea salt; (b) ammonium sulphate; (c) soil 1; (d) nitrate aerosol/traffic 2. (The black dot indicates the location of sampling point).

located in North Africa (Fig. 4a.1). Low-pressure systems in the Atlantic can on occasion have the same effect (see Fig. 4a.2).

Likewise, two noteworthy zones obtained moderately high PSCF values (between 0.45–0.65) for the soil 1 source. The first is in northeastern Algeria, the Mediterranean coast near it and Tunisia, with the second being western Algeria and Morocco (Fig. 3c). These zones are related to Saharan dust intrusions in the study area, and the predominant synoptic situation is high pressure located between the Mediterranean and North Africa. Concerning the latitude of the centre of the anticyclone, the particulate matter originates from either one zone or the other (see Figs. 4b.1 and b.2). Note that the origin of African dust arriving at the study area derives from the seasonality in the synoptic scenarios. According to Escudero et al. (2005), there are four meteorological situations that originate the transport of dusty African air masses towards the Western Mediterranean basin.

The secondary nitrate/traffic 2 source has two potential areas that stand out. The first and most extensive is located in east-central France, southern Switzerland and northern Italy (Fig. 3d). An increase in the residence time of backtrajectories could pos-

sibly extend this potential zone all the way to Germany. These central European zones are considered important source areas of nitrogen oxides emissions in Europe (Duyzer and Fowler, 1994). The second area is found in northern Algeria.

The bulk of days whose concentrations exceed the 75th percentile for this source are related to local pollution episodes. The synoptic situations under which the majority of these episodes take place are in the winter period, anticyclonic and calm (Fig. 4c.1). However, some (~27%) are associated with long-range transport from central Europe. The meteorological pattern usually presenting this type of transport is that of low pressure centred in Italy (Fig. 4c.2).

PSCF analysis was also applied to PM<sub>2.5</sub> (Fig. 5). This map shows two important features:

(1) The potential source areas are located to the south (Morocco and northwestern Algeria) and west (Atlantic Ocean between the latitudes 34–38°N) of the sampling point. The fact that neither continental European nor Mediterranean influence was registered is possibly due to the important contribution (NH<sub>4</sub>)<sub>2</sub>SO<sub>4</sub> has upon PM<sub>2.5</sub>.



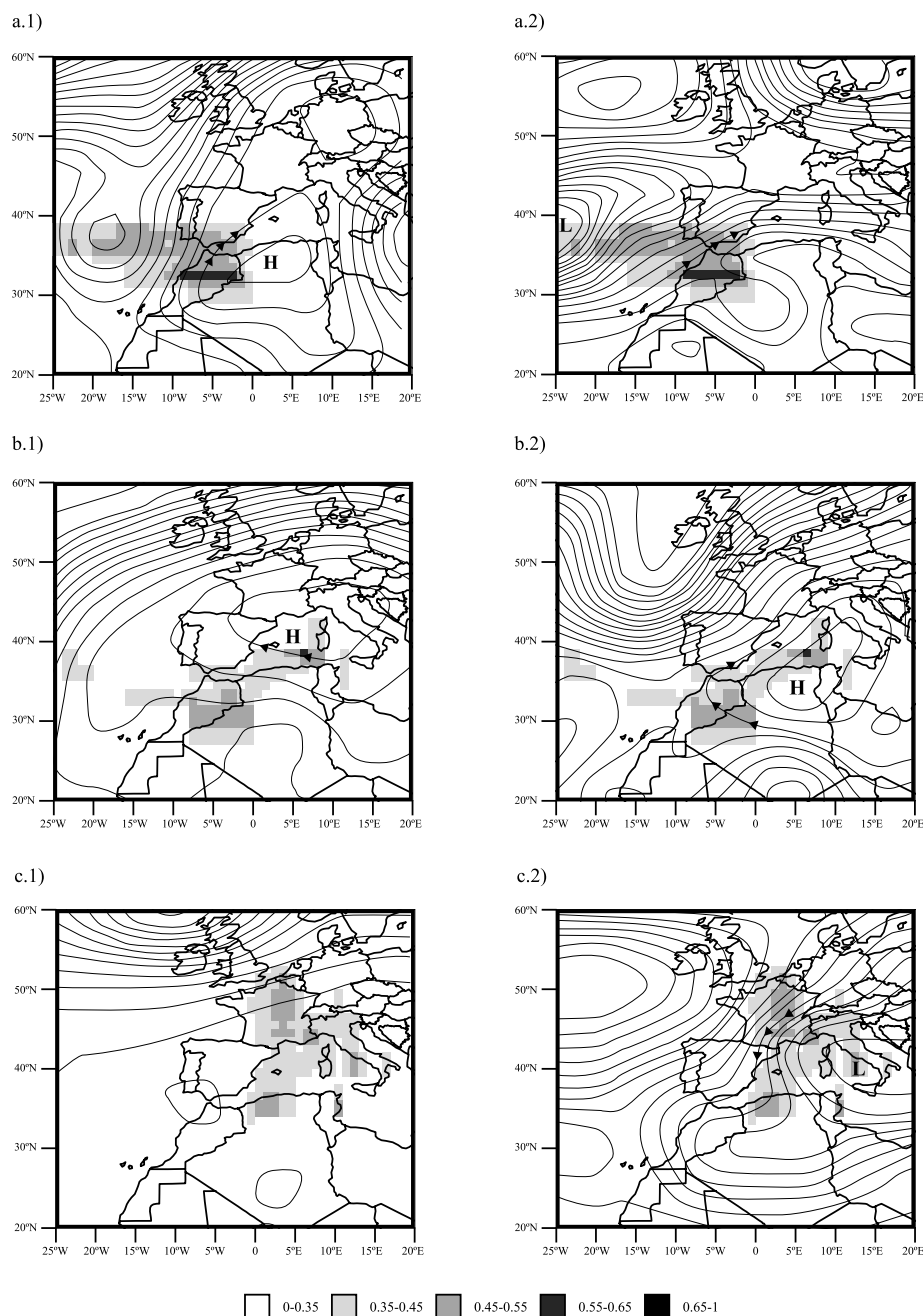


Fig. 4. Meteorological situations determined at 850 mb geopotential height at 18:00 UTC, under which the trajectories of air masses arriving to the sampling point either originate in or pass through zones with moderate or high PSCF levels: (a.1) and (a.2) ammonium sulphate; (b.1) and (b.2) soil 1; (c.1) and (c.2) nitrate aerosol/traffic 2.

(2) The PSCF values in these source areas are moderate, not exceeding 0.55.

## 5. Conclusions

Based on the results obtained from the analysis (composition, sources and potential regions) performed on the fine fraction in

the city of Elche (southeastern Spain), the following conclusions can be drawn:

(1) Both the temporal variability as much as the maximum annual values registered for  $PM_{2.5}$  are conditioned upon the temporal succession of pollution episodes of local character and upon the arrival of Saharan air masses. In this last case, the

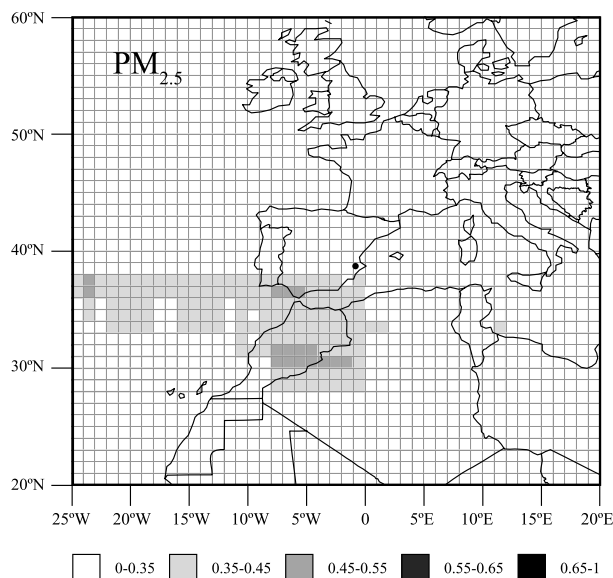


Fig. 5. PSCF values for PM<sub>2.5</sub>. (The black dot indicates the location of sampling point).

multivariate analysis carried out reflects the contribution these long-distance events have upon PM<sub>2.5</sub> in the study area.

(2) The role ammonium sulphate plays in the fine fraction is exceptional, as its annual average contribution has been estimated around 40%. Furthermore, this compound manages to modulate the seasonal variability of PM<sub>2.5</sub>, even in winter.

(3) Source regions for non-local components of PM<sub>2.5</sub> are located in the Atlantic and northwestern continental Africa (primarily Morocco and northwestern Algeria), with the exception of the nitrate aerosol/traffic 2 source, to which a European origin can be partially assigned. These results indicate that European influence at the sampling point is minimal.

## Acknowledgments

We thank the Elche City hall for allowing access to their facilities for the placement of the instruments, the Air Quality Surveillance Network of the Valencian Community Regional Government for supplying data.

## References

- Almeida, S., Pio, C., Freitas, M., Reis, M. and Trancoso, M. 2006. Source apportionment of atmospheric urban aerosol based on week-days/weekend variability: evaluation of road re-suspended dust contribution. *Atmos. Environ.* **40**, 2058–2067.
- Ara Begum, B., Kim, E., Jeong, C.-H., Lee, D.-W. and Hopke, P.K. 2005. Evaluation of potential source contribution function using the 2002 Quebec forest fire episode. *Atmos. Environ.* **39**, 3719–3724.
- Ashbaugh, L.L., Malm, W.C. and Sadeh, W.D. 1985. A residence time probability analysis of sulfur concentrations at Grand Canyon National Park. *Atmos. Environ.* **19**, 1263–1270.
- Calzolai, G., Chiari, M., García Orellana, I., Lucarelli, F., Migliori, A. and co-authors. 2006. The new external beam facility for environmental studies at the Tandatron accelerator of LABEC. *Nucl. Instrum. Methods Phys. Res., Sect. B* **249**, 928–931.
- Dockery, D.W., Pope, C.A., Xu, X.P., Spengler, J.D., Ware, J.H. and co-authors. 1993. An association between air pollution and mortality in six U.S. cities. *N. Engl. J. Med.* **329**, 1753–1759.
- Doğan, G., Güllü, G. and Tuncel, G. 2008. Sources and source regions effecting the aerosol composition of the Eastern Mediterranean. *Microchem. J.* **88**, 142–149.
- Draxler, R.R. and Rolph, G.D. 2010. HYSPLIT (Hybrid Single-Particle Lagrangian Integrated Trajectory). Model access via NOAA ARL READY website (<http://ready.arl.noaa.gov/HYSPLIT.php>). NOAA Air Resources Laboratory, Silver Spring, MD.
- Duyzer, J. and Fowler, D. 1994. Modelling land atmosphere exchange of gaseous oxides of nitrogen in Europe. *Tellus* **46 B**, 353–372.
- Escudero, M., Castillo, S., Querol, X., Avila, A., Alarcon, M. and co-authors. 2005. Wet and dry African dust episodes over Eastern Spain. *J. Geophys. Res.* **110**, 4731–4746.
- Galindo, N., Nicolás, J. F., Yubero, E., Caballero, S., Pastor, C. and co-authors. 2008. Factors affecting levels of aerosol sulfate and nitrate on the Western Mediterranean coast. *Atmos. Res.* **88**, 305–313.
- Götschi, T., Hazenkamp, M. E., Heinrich-von-Arx, J., Bono, R., Burney, P., Forsberg, B. and co-authors. 2005. Elemental composition and reflectance of ambient fine particles at 21 European locations. *Atmos. Environ.* **39**, 5947–5958.
- Hazenkamp-von Arx, M. E., Götschi, T., Ackermann-Liebrich, U., Bono, R., Burney, P. and co-authors. 2004. PM<sub>2.5</sub> and NO<sub>2</sub> assessment in 21 European study centres of ECRHS II: annual means and seasonal differences. *Atmos. Environ.* **38**, 1943–1953.
- Hwang, I. and Hopke, P. H. 2007. Estimation of source apportionment and potential source locations of PM<sub>2.5</sub> at a west coastal IMPROVE site. *Atmos. Environ.* **41**, 506–518.
- Kalnay, E., Kanamitsu, M., Kistler, R., Collins, W., Deaven, D. and co-authors. 1996. The NCEP/NCAR 40-year reanalysis project. *Bull. Am. Meteorol. Soc.* **77**, 437–471.
- Kaneyasu, N., Yoshikado, H., Mizuno, T., Sakamoto, K. and Soufuku, M. 1999. Chemical forms and sources of extremely high nitrate and chloride in winter aerosol pollution in the Kanto Plain of Japan. *Atmos. Environ.* **33**, 1745–1756.
- Kim, E., Hopke, P. K. and Edgerton, E. S. 2004. Improving source identification of Atlanta aerosol using temperature resolved carbon fractions in positive matrix factorization. *Atmos. Environ.* **38**, 3349–3362.
- Kim, E., Larson, T. V., Hopke, P. H., Slaughter, C., Sheppard, L. E. and co-authors. 2003. Source identification of PM<sub>2.5</sub> in an arid Northwest U.S. City by positive matrix factorization. *Atmos. Res.* **66**, 291–305.
- Koçak, M., Mihalopoulos, N. and Kubilay N. 2009. Origin and source regions of PM<sub>10</sub> in the Eastern Mediterranean atmosphere. *Atmos. Res.* **92**, 464–474.
- Kuhns, H., Bohdan, V., Chow, J. C., Etyemezian, V., Green, M. C. and co-authors. 2003. The Treasure Valley secondary aerosol study I: measurements and equilibrium modeling of inorganic secondary aerosols and precursors for southwestern Idaho. *Atmos. Environ.* **37**, 511–524.

- McClain, C. R., Cleave, M. L., Feldman, G. C., Gregg, W. W., Hooker, S. B. and co-authors. 1998. Science quality SeaWiFS data for global biosphere research. *Sea Technol.* **39**, 10–16.
- Nickovic, S., Papadopoulos, A., Kakaliagou, O. and Kallos, G. 2001. Model for prediction of desert dust cycle in the atmosphere. *J. Geophys. Res.* **106**, 18113–18129.
- Nicolás, J. F., Chiari, M., Crespo, J., Garcia Orellana, I., Lucarelli, F. and co-authors. 2008. Quantification of Saharan and local dust impact in an arid Mediterranean area by the positive matrix factorization (PMF) technique. *Atmos. Environ.* **42**, 8872–8882.
- Paatero, P. 1997. Least squares formulation of robust non-negative factor analysis. *Chemom. Intell. Lab. Syst.* **38**, 223–242.
- Paatero, P. 2004. *User's Guide for Positive Matrix Factorization Programs PMF2 and PMF3. Part. 1: Tutorial*. University of Helsinki, Department of Physics, Finland.
- Paatero, P. and Tapper, U. 1994. Positive matrix factorization: a non-negative factor model with optimal utilization of error estimates of data values. *Environmetrics* **5**, 111–126.
- Perrino, C., Catrambone, M. and Pietrodangelo, A. 2008. Influence of atmospheric stability on the mass concentration and chemical composition of atmospheric particles: a case study in Rome, Italy. *Environ. Int.* **34**, 621–628.
- Plaisance, H., Coddeville, P., Roussel, I. and Guillermo, R. 1996. A qualitative determination of the source locations of precipitation constituents in Morvan, France. *Environ. Technol.* **17**, 977–986.
- Polissar, A. V., Hopke, P. K. and Harris, J. M. 2001. Source regions for atmospheric aerosol measured at Barrow, Alaska. *Environ. Sci. Technol.* **35**, 4214–4226.
- Polissar, A. V., Hopke, P. K., Malm, W. C. and Sisler, J. F. 1998. Atmospheric aerosol over Alaska-2. Elemental composition and sources. *J. Geophys. Res.* **103**(D15), 19045–19057.
- Querol, X., Alastuey, A., Moreno, T., Viana, M. M., Castillo, S. and co-authors. 2008. Spatial and temporal variations in airborne particulate matter (PM<sub>10</sub> and PM<sub>2.5</sub>) across Spain 1999–2005. *Atmos. Environ.* **42**, 3964–3979.
- Querol, X., Alastuey, A., Ruiz, C. R., Artiñano, B., Hansson, H. C. and co-authors. 2004. Speciation and origin of PM<sub>10</sub> and PM<sub>2.5</sub> in selected European cities. *Atmos. Environ.* **38**, 6547–6555.
- Salvador, P., Artiñano, B., Alonso, D., Querol, X. and Alastuey, A. 2004. Identification and characterisation of sources of PM<sub>10</sub> in Madrid (Spain) by statistical methods. *Atmos. Environ.* **38**, 435–447.
- Salvador, P., Artiñano, B., Querol, X. and Alastuey, A. 2008. A combined analysis of backward trajectories and aerosol chemistry to characterize long-range transport episodes of particulate matter: the Madrid air basin, a case study. *Sci. Total Environ.* **390**, 495–506.
- Schaap, M., van Loon, M., ten Brink, H. M., Dentener, F. J. and Builtjes, P. J. H. 2004. Secondary inorganic aerosol simulations for Europe with special attention to nitrate. *Atmos. Chem. Phys.* **4**, 857–874.
- Schwartz, J. and Neas, L. 2000. Fine particles are more strongly associated than coarse particles with acute respiratory health effects in schoolchildren. *Epidemiology* **11**, 6–10.
- Sternbeck, J., Sjödin, A. and Andréasson, K. 2002. Metal emissions from road traffic and the influence of resuspension-results from two tunnel studies. *Atmos. Environ.* **36**, 4735–4744.
- Stohl, A. 1996. Trajectory statistics: a new method to establish source–receptor relationships of air pollutants and its application to the transport of particulate sulfate in Europe. *Atmos. Environ.* **30**, 579–587.
- Thorpe, A. and Harrison, R. M. 2008. Sources and properties of non-exhaust particulate matter from road traffic: a review. *Sci. Total Environ.* **400**, 270–282.
- Thurston, G. D. and Spengler, J. D. 1985. A quantitative assessment of source contribution to inhalable particulate matter pollution in Metropolitan Boston. *Atmos. Environ.* **19**, 9–25.
- Viana, M., Querol, X., Götschi, T., Alastuey, A., Sunyer, J. and co-authors. 2007. Source apportionment of ambient PM<sub>2.5</sub> at five Spanish centers of European community respiratory health survey (ECRHS II). *Atmos. Environ.* **41**, 1395–1406.